

Preface

A tool for Integrated District Energy Assessment by Simulation (IDEAS) is developed and allows integrated transient simulation of thermal and electrical processes at neighborhood level. The IDEAS tool differs from existing BPS-based and EES-based models by (i) integrating the dynamics of the hydronic, thermal as well as electrical energy networks at (ii) both the building and aggregated level within a single model and solver.

The present document contains the complete specifications of the IDEAS tool. All equations are written in such way that positive energy flows increase the energy of the specific system. Unless stated differently, all variables are measured in SI units, i.e. length in meter and mass in kilogram. An exception is made for temperature where T depicts the absolute temperature in Kelvin and ϑ in degrees Celcius.

Leuven,
January 2012

*Ruben Baetens
Roel De Coninck
Juan Van Roy
Bart Verbruggen*

Contents

Part I Specifications

1	Climate	3
	Ruben Baetens and Dirk Saelens	
1.1	Weather data	3
1.2	Solar radiation	4
1.2.1	Solar geometry	5
1.2.2	Shortwave radiation on a tilted surface	6
2	Transient building response model	9
	Ruben Baetens and Dirk Saelens	
2.1	Wall response model	9
2.1.1	Exterior surface heat balance	10
2.1.2	Wall conduction process	10
2.1.3	Interior surface heat balance	11
2.1.4	Model extension for windows	13
2.1.5	Model extension for ground slabs	14
2.2	Zone model	15
2.2.1	Thermal response model	15
2.2.2	Thermal comfort	16
2.3	Initial value problem	17
3	Thermal building system	19
	Roel De Coninck and Lieve Helsen	
4	Electricity system	21
	Juan Van Roy, Bart Verbruggen and Johan Driesen	

Part II Validation or verification

5	Building energy simulation test - BESTEST	25
	Ruben Baetens and Dirk Saelens	
5.1	Introduction	25

5.1.1	Building energy simulation test cases	25
5.1.2	Test results	26
6	Thermal building energy system test - BESTEST	29
	Roel De Coninck and Lieve Helsen	
7	IEEE Distribution system analysis for radial test feeders	31
	Juan Van Roy, Bart Verbruggen and Johan Driesen	
Part III Literature		
	Bibliography	35
	Index	37

List of Contributors

Ruben Baetens

K.U.Leuven, Kasteelpark Arenberg 40 bus 2447, BE-3001 Leuven (Heverlee) e-mail:
ruben.baetens@bwk.kuleuven.be

Roel De Coninck

K.U.Leuven, Celestijnenlaan 300a bus 2421, BE-3001 Leuven (Heverlee) e-mail:
roel.deconinck@mech.kuleuven.be

Juan Van Roy

K.U.Leuven, Kasteelpark Arenberg 10 bus 2445, BE-3001 Leuven (Heverlee) e-mail:
juan.vanroy@esat.kuleuven.be

Bart Verbruggen

K.U.Leuven, Kasteelpark Arenberg 10 bus 2445, BE-3001 Leuven (Heverlee) e-mail:
bart.verbruggen@esat.kuleuven.be

Johan Driesen

K.U.Leuven, Kasteelpark Arenberg 10 bus 2445, BE-3001 Leuven (Heverlee) e-mail:
johan.driesen@esat.kuleuven.be

Lieve Helsen

K.U.Leuven, Celestijnenlaan 300a bus 2421, BE-3001 Leuven (Heverlee) e-mail:
lieve.helsen@mech.kuleuven.be

Dirk Saelens

K.U.Leuven, Kasteelpark Arenberg 40 bus 2447, BE-3001 Leuven (Heverlee) e-mail:
dirk.saelens@bwk.kuleuven.be

Part I

Specifications

spec-i-fi-ca-tion (n.) 1. the act of specifying. 2. a. specifications, A detailed, exact statement of particulars, especially a statement prescribing materials, dimensions, and quality of work for something to be built, installed, or manufactured. b. A single item or article that has been specified. 3. An exact written description of an invention by an applicant for a patent.

Chapter 1

Climate

Ruben Baetens and Dirk Saelens

Abstract A numeric building model is developed in Modelica for integrated energy simulation.

In this section, we describe in detail the climate model and its possibilities that are implemented in Modelica as part of the IDEAS platform. Four external factors are to be known, i.e. external temperature and ground temperature for transient heat losses by conduction, sky temperature for long-wave radiation losses and short-wave gains on surfaces by solar irradiation.

1.1 Weather data

Within the computational model, all weather data are handled in

determined by `city` depicting the location of the used climate determined by its latitude and longitude as well as design climate data for system design, and `detail` depicting the time resolution of the used data.

The main weather parameters required for transient thermal building simulation are the ambient dry-bulb temperature $T_{db}(t)$, the outdoor relative humidity $\phi_e(t)$, the wind speed $v_{10}(t)$, the diffuse horizontal solar radiation $E_{d,h}(t)$ and direct normal solar radiation $E_{D,\perp}(t)$.

The Meteonorm system [?] is a comprehensive source of (all mentioned) weather data for engineering applications in Europe and this system is used within this context. For simulation, the retrieved data from the Meteonorm system are not used within the common formats of a test reference year `*.try` [?, ?] as used in Europe or the formats of a typical meteor-

Ruben Baetens

K.U.Leuven, Kasteelpark Arenberg 40 bus 2447, BE-3001 Leuven (Heverlee) e-mail: ruben.baetens@bwk.kuleuven.be

Dirk Saelens

K.U.Leuven, Kasteelpark Arenberg 40 bus 2447, BE-3001 Leuven (Heverlee) e-mail: dirk.saelens@bwk.kuleuven.be

logical years `*.tmy` or `*.tmy2` [?, ?] and weather years for energy calculations `*.wyec` or `*.wyec2` [?] as used in the United States and Canada. These data formats are derived from hourly observations at a specific location by the national weather service or meteorological office and contain too little information for sub-hourly simulation, especially towards renewable energy generation by solar radiation.

From the retrieved data from the Meteonorm system, one more temperature needs to be determined. The long-wave radiative heat exchange of an exterior surface with a cloudy sky is calculated based on a sky temperature. This black-body sky temperature $T_{sky}(t)$ can be determined [?, ?] as

$$T_{sky}(t) = T_{db}(t) \epsilon_{sky}(t)^{0.25} \quad (1.1)$$

$$\epsilon_{sky}(t) = \epsilon_0(t) + \Delta\epsilon_h(t) + CCF(t) [1 - \epsilon_h(t) - \Delta\epsilon_h(t)] \quad (1.2)$$

where $\epsilon_{sky}(t)$ is the cloudy sky emissivity [?, ?, ?], where $\epsilon_0(t) + \Delta\epsilon_h(t)$ is the clear sky emissivity $\epsilon_{clear}(t)$, $\Delta\epsilon_h(t)$ is a diurnal correction taking into account the difference in sky emissivity between day and night and $CCF(t)$ is the cloud cover factor. Both $\epsilon_{clear}(t)$ and $CCF(t)$ are determined as polynomial fits on measurement data:

$$\epsilon_0(t) + \Delta\epsilon_h(t) = 0.711 + 0.0056 \vartheta_{dew}(t) + 0.000073 \vartheta_{dew}(t)^2 + 0.013 \cosh(t) \quad (1.3)$$

$$CCF(t) = 1.0 + 0.024 CC(t) - 0.0035 CC(t)^2 + 0.00028 CC(t)^3 \quad (1.4)$$

where $h(t)$ is the hour angle, $\vartheta_{dew}(t)$ is the dew temperature and $CC(t)$ is the tenths cloud cover retrieved from Meteonorm [?, ?].

1.2 Solar radiation

The calculation of the direct and diffuse solar irradiation on a tilted surface requires determination of the position of the sun in the sky. Here, the zenith angle $\xi(t, x)$ of surface with inclination $i(x)$ and azimuth $a(x)$ are able to uniquely define the solar radiation on a tilted surface based on the determination of the annual and daily solar cycle by means of solar time and declination.

Within the computational model, all solar irradiation calculations are handled in `Commons.Meteo.Solar.RadSol` which is built-in in each surface receiving solar radiation.

1.2.1 Solar geometry

The *apparent solar time* $t_{sol}(t)$ expressed in seconds is based on daily apparent motion of the sun as seen from the earth. Solar noon is defined as the moment when the sun reaches the highest point in the sky. Solar time defined as

$$t_{sol}(t) = t_{std}(t) + 720\pi^{-1} [L_{std} - L_{loc}] + E_t(t) \quad (1.5)$$

$$E_t(t) = -120 e \sin M(t) + 60 \tan^2(\varepsilon/2) \sin(2M(t) + 2\lambda_p) \quad (1.6)$$

where $t_{std}(t)$ is the standard time of the time zone, L_{std} is the reference meridian, L_{loc} is the local meridian and E_t is the *equation of time* defining the difference between solar noon and noon of local civil time, $M(t)$ is the mean anomaly relating to the position of the sun to the earth in a Kepler orbit, ε is the earth obliquity and λ_p the ecliptic longitude of the periaapsis, i.e. the closest approach of the earth to the sun.

Daylight saving time is taken into account within the simulation and corrects $t_{std}(t)$. Daylight saving time starts in the *European Economic Community* on March $31 - [(5y)/4 + 4] \bmod 7$ and ends on October $31 - [(5y)/4 + 1] \bmod 7$ where y denotes the year and \bmod denotes the remainder by division [?].

Before the zenith angle can be calculated, the declination δ and solar hour angle $h(t)$ is to be defined to fully specify the position of the sun as seen by an observer at a given time. Here, $\delta(t)$ depicts the angle between the solar beam and the equatorial plane, defined [?] as

$$\sin \delta(t) = \sin \varepsilon \cos(2\pi(n(t) + 10)n_y^{-1}) \quad (1.7)$$

where ε is the earth obliquity, $n(t)$ is the one-based day number, i.e. 1 for January 1, and n_y is the length in days of the earth revolution equal to 365.25 days. The correction of 10 days is required as winter solstice, i.e. when the apparent position of the sun in the sky as viewed from the Earth reaches its most northern extreme, occurs at December 21.

The hour angle $h(t)$ depicts the angle between between the half plane of the Earth's axis and the zenith and the half plane of the Earth's axis and the given location, defined as

$$h(t) = 2\pi t_{sol}(t) 86400^{-1} - \pi \quad (1.8)$$

where $t_{sol}(t)$ is solar time.

Based on $\delta(t)$ and $h(t)$, the zenith angle $\xi(t, x)$ of a surface with inclination $i(x)$ and azimuth $a(x)$ can be uniquely defined. The zenith angle of the sun to a surface is the angle between this surface normal and the sun's beam, and is derived from [?, ?]

$$\begin{aligned} \cos \xi(t, x) = & \sin \delta(t) \sin \varphi \cos i(x) - \sin \delta(t) \cos \varphi \sin i(x) \cos a(x) \\ & + \cos \delta(t) \cos \varphi \cos i(x) \cos a(x) \\ & + \cos \delta(t) \cos h(t) \sin \varphi \sin i(x) \cos a(x) + \cos \delta(t) \sin h(t) \sin i_s \sin a(x) \end{aligned} \quad (1.9)$$

where φ is the latitude of the location defined positive for the northern hemisphere, $h(t)$ is the hour angle, $i(x)$ is the surface inclination defined as 0 for ceilings and $\pi/2$ for vertical

walls, $a(x)$ is the surface azimuth defined as $-\pi/2$ if the surface outward normal points eastward and 0 if the normal points southward, and where $\delta(t)$ is the solar declination.

1.2.2 Shortwave radiation on a tilted surface

The total solar irradiation $E(t, x)$ on a arbitrary surface can be determined as the sum of the direct $E_D(t, x)$, diffuse $E_d(t, x)$ and reflected $E_r(t, x)$ radiation on the surface.

$$E(t, x) = E_D(t, x) + E_d(t, x) + E_r(t, x) \quad (1.10)$$

For a known profile of direct solar irradiation on a random surface, all three factors can be determined for another arbitrary surface s . Herefore, a profile of direct solar irradiation $E_{D,\perp}(t, x)$ perpendicular on the beam radiation is retrieved from Meteonorm and used as only input parameter. The calculation of other configurations besides normal to the solar beam is performed in the model.

Different models [?] for the determination of the diffuse radiation do exist based on an isotropic [?, ?, ?] or anisotropic [?, ?, ?, ?, ?, ?, ?, ?] model of the sky dome. On account of the high importance of solar irradiation for the model (i.e. for the building thermal response, heat generation by means of a thermal solar collector and power generation with a photovoltaic array), a more detailed determination of diffuse radiation based on a anisotropic sky dome model is favorable. Herefore, the model presented by Skartveit and Olseth [?] is implemented and choosen above the Perez model [?, ?] as it is based on analytical expressions and does not resort to extensive look-up tables.

$$E(t, x) = r_D(t, x)E_{D,h}(t) + r_d(t, x)E_{d,h}(t) + F_r(t, x)\rho(t) [E_{D,h}(t) + E_{d,h}(t)] \quad (1.11)$$

wherefore $r_D(t, x)$ and $r_d(t, x)$ are the ratios between direct and diffuse radiation respectively on a tilted surface to that on a horizontal surface, defined as

$$r_D(t, x) = \cos \xi(t, x) \cos^{-1} \xi_h(t) \quad (1.12)$$

$$r_d(t, x) = r_D(t, x) \frac{E_{D,h}(t)}{E_{oh}(t)} + \Omega(t) \cos i(x) + F_d(t, x) \left[1 - \frac{E_{D,h}(t)}{E_{oh}(t)} - \Omega(t) \right] \quad (1.13)$$

and wherefore $\xi(t, x)$ and $\xi_h(t)$ are the zenith angle for surface s and the horizontal surface respectively, i.e. the angle between the straight line joining the centers of the earth and the sun and the normal of surface s , ρ is the albedo, i.e. the average reflectivity of the environment, $E_{oh}(t)$ is the total extraterrestrial solar irradiation, $i(x)$ is the surface inclination defined as 0 for flat roofs and $\pi/2$ for vertical walls, $\Omega(t)$ equals $\max \{0, 0.3 - 2E_{D,h}(t)/E_{oh}(t)\}$, $F_r(t, x)$ is the isotropic reflected view factor defined as $[1 - \cos \xi(t, x)]/2$ and $F_d(t, x)$ is the isotropic diffuse view factor defined as $[1 + \cos \xi(t, x)]/2$.

For calculation of the reflected solar irradiation $E_r(t, x)$, the albedo $\rho(t)$ is determined [?] as

$$\rho(t) = 11.895 - 0.042 T_{db}(t), \forall \rho(t) \in [0.2, 0.8] \quad (1.14)$$

where $T_{db}(t)$ is the average outdoor dry-bulb temperature of the last two weeks.
The total extraterrestrial solar irradiation $E_{oh}(t)$ is defined as [?]

$$E_{oh}(t) = S_{sol} + 0.033412 S_{sol} \cos d(t) \quad (1.15)$$

where $d(t)$ is day angle and S_{sol} is the solar constant [?] equaling 1366.1 Wm^{-2} .

Chapter 2

Transient building response model

Ruben Baetens and Dirk Saelens

Abstract A numeric building model is developed in Modelica for integrated energy simulation.

In this section, we describe in detail the dynamic building model and its possibilities that are implemented in Modelica as part of the IDEAS platform. The building model allows simulation of the energy demand for heating and cooling of a multi-zone building, energy flows in the building envelope and interconnection with dynamic models of thermal and electrical building energy systems within the IDEAS platform for comfort measures.

The description is divided into the description of the model and the model. The window model and the model for ground losses are described more in detail as extend to the wall model.

The relevant material properties of the surfaces are complex functions of the surface temperature, angle and wavelength for each participating surface. The assumptions used frequently in engineering applications [?] are that (i) each surface emits or reflects diffusely, that (ii) each surface is at a uniform temperature, that (iii) the energy flux leaving a surface is evenly distributed across the surface and (iv) is one-dimensional.

2.1 Wall response model

The description of the thermal response of a (or a structure of parallel opaque layers in general) is structured as in the 3 different occurring processes, i.e. the heat balance of the exterior surface, heat conduction between both surfaces and the heat balance of the interior surface.

Ruben Baetens

K.U.Leuven, Kasteelpark Arenberg 40 bus 2447, BE-3001 Leuven (Heverlee) e-mail: ruben.baetens@bwk.kuleuven.be

Dirk Saelens

K.U.Leuven, Kasteelpark Arenberg 40 bus 2447, BE-3001 Leuven (Heverlee) e-mail: dirk.saelens@bwk.kuleuven.be

2.1.1 Exterior surface heat balance

The heat balance of the exterior surface is determined as

$$Q_{net}(t, x) = Q_c(t, x) + Q_{SW}(t, x) + Q_{LW,e}(t, x) + Q_{LW,sky}(t, x) \quad (2.1)$$

where $Q_{net}(t, x)$ denotes the heat flow into the wall, $Q_c(t, x)$ denotes heat transfer by convection, $Q_{SW}(t, x)$ denotes short-wave absorption of direct and diffuse solar light, $Q_{LW,e}(t, x)$ denotes long-wave heat exchange with the environment and $Q_{LW,sky}(t, x)$ denotes long-wave heat exchange with the sky.

Convection. The exterior convective heat flow $Q_c(t, x)$ is computed as

$$Q_c(t, x) = 5.01 v_{10}(t)^{0.85} A(x) [T_{db}(t) - T_s(t, x)] \quad (2.2)$$

where $A(x)$ is the surface area, $T_{db}(t)$ is the dry-bulb exterior air temperature, $T_s(t, x)$ is the surface temperature and $v_{10}(t)$ is the wind speed in the undisturbed flow at 10 meter above the ground and where the stated correlation is valid for a v_{10} range of $[0.15, 7.5]$ meter per second [?]. The $v_{10}(t)$ -dependent term denoting the exterior convective heat transfer coefficient $h_{ce}(t)$ is determined as $\max\{f(v_{10}), 5.6\}$ in order to take into account buoyancy effects at low wind speeds [?].

Longwave radiation. Longwave radiation between the surface and environment $Q_{LW,e}(x)$ is determined as

$$Q_{LW,e}(t, x) = \sigma \epsilon_{LW}(x) A(x) [T_s(t, x)^4 - F_{sky}(x) T_{sky}(t)^4 - (1 - F_{sky}(x)) T_{db}(t)^4] \quad (2.3)$$

as derived from the Stefan-Boltzmann law [?, ?] wherefore σ the Stefan-Boltzmann constant [?], $\epsilon_{LW}(x)$ the longwave emissivity of the exterior surface, $A(x)$ is the surface area, $F_{sky}(x)$ the radiant-interchange configuration factor between the surface and sky [?] as defined on page 4, and the surface and the environment respectively and $T_s(t, x)$ and $T_{sky}(t)$ are the exterior surface and sky temperature respectively.

Shortwave radiation. Shortwave solar irradiation absorbed by the exterior surface $Q_{SW}(t, x)$ is determined as $\epsilon_{SW}(x) A(x) E_S(t, x)$ where $\epsilon_{SW}(x)$ is the shortwave absorption of the surface, $A(x)$ the surface area and $E_S(t, x)$ the total irradiation on the depicted surface. The calculation method for solar irradiation $E_S(t, x)$ depending on latitude, time, weather conditions, inclination and orientation is described in detail on page 4.

2.1.2 Wall conduction process

For the purpose of dynamic building simulation, the partial differential equation of the continuous time and space model of heat transport through a solid is most often simplified into ordinary differential equations with a finite number of parameters representing only one-dimensional heat transport through a construction layer. Within this context, the wall is mod-

eled with lumped elements, i.e. a model where temperatures and heat fluxes are determined from a system composed of a sequence of discrete resistances and capacitances R_{n+1} , C_n . The number of capacitive elements n used in modeling the transient thermal response of the denotes the order of the lumped capacitance model.

$$Q_{net}(t, w) = \frac{\partial T_c(t, w)}{\partial t} C(x) = \sum_i^n Q_{res,i}(t, x) + Q_{source}(t, x) \quad (2.4)$$

where $dQ_{net}(t, x)$ is the added energy to the lumped capacity, $T_c(t, x)$ is the temperature of the lumped capacity, $C_c(x)$ is the thermal capacity of the lumped capacity equal to $\rho(x)c(x,t)d_cA(x)$ for which $\rho(x)$ denotes the density and $c(x)$ is the specific heat capacity of the material, d_c the equivalent thickness of the lumped element and $A(x)$ the surface of the modeled layer, where $Q_{res}(t, x)$ the heat flux through the lumped resistance and $R_r(x)$ is the total thermal resistance of the lumped resistance equal to $d_r(\lambda(x,t)A(x))^{-1}$ for which d_r denotes the equivalent thickness of the lumped element and where Q_{source} are internal thermal source, e.g. from embedded systems.

Studies on the optimal order reduction for lumped construction elements in thermal building models can be found in literature [?, ?, ?, ?, ?], where optimization towards reduction is performed through comparison of zone air temperatures or comparison of Bode plots [?] on magnitude and phase for the low-order and a high-order lumped element. The general conclusion found towards model accuracy and computational efficiency depict that 1st-order lumped elements do not seem to be able to deal with radiation on the surfaces whereas 2nd-order lumped elements, i.e. based on two capacities and three resistances, give minimal loss of accuracy compared to high-order reference models for a limited computational effort. Both light and medium constructions [?] show high accuracy if a 2nd-order lumped element is used and little improvements can be achieved through optimization on nodal placement [?, ?, ?, ?] whereas a higher order thermal network should be used for heavy constructions [?] when the dynamics of the system are of concern as significant errors remain for simplified models at low frequency [?, ?, ?].

The model has a provision for including a temperature coefficient $f_{\lambda,c}$ to modify the thermal conductivity. The general description for the temperature dependency of the material thermal conductivity λ is $\lambda_0 + f_{\lambda,c}[T_C - T_0]$ where T_0 is the temperature for which the standard input thermal conductivity is defined at standard temperature and pressure (STP) conditions. If $f_{\lambda,c}$ is not defined, no temperature dependence is taken into account and set to unity.

2.1.3 Interior surface heat balance

The heat balance of the interior surface is determined as

$$Q_{net}(t, x) = Q_c(t, x) + \sum_i^N Q_{SW,i}(t, x) + \sum_i^N Q_{LW,i}(t, x) \quad (2.5)$$

where $Q_{net}(t, x)$ denotes the heat flow into the wall, $Q_c(t, x)$ denotes heat transfer by convection, $Q_{SW}(t, x)$ denotes short-wave absorption of direct and diffuse solar light netting the interior zone through windows and $Q_{LW,i}(t, x)$ denotes long-wave heat exchange with the surrounding interior surfaces.

Convection. The surface heat resistances $R_s(t, x)$ for the exterior and interior surface respectively are determined as $R_s(t, x)^{-1} = A(x)h_c(t, x)$ where $A(x)$ is the surface area and where $h_c(t, x)$ is the exterior and interior convective heat transfer coefficient. The interior natural convective heat transfer coefficient $h_{ci}(t, x)$ is computed for each interior surface as

$$h_{ci}(t, x) = n_1(t, x)D(x)^{n_2(t, x)} |T_a(t, x) - T_s(t, x)|^{n_3(t, x)} \quad (2.6)$$

where $D(x)$ is the characteristic length of the surface, $T_a(t, x)$ is the indoor air temperature $T_s(t, x)$, and $n_i(t, x)$ are correlation coefficients. These parameters $\{n_1, n_2, n_3\}$ are identical to $\{1.823, -0.121, 0.293\}$ for vertical surfaces [?], $\{2.175, -0.076, 0.308\}$ for horizontal surfaces wherefore the heat flux is in the same direction as the buoyancy force [?], and $\{2.72, -, 0.13\}$ for horizontal surfaces wherefore the heat flux is in the opposite direction as the buoyancy force [?]. The interior natural convective heat transfer coefficient is only described as function of the temperature difference. An overview of a more detailed correlation including the possible higher wind velocities due to mechanical ventilation can be found in literature [?] but are not implemented.

Longwave radiation. Similar to the thermal model for heat transfer through a wall, a thermal circuit formulation for the direct radiant exchange between surfaces can be derived [?, ?, ?]. The resulting heat exchange by longwave radiation between two surface s_i and s_j can be described as

$$Q_{s_i, s_j}(t) = \sigma \left[\frac{1 - \epsilon_{s_i}}{\epsilon_{s_i}} + \frac{1}{F_{s_i, s_j}} + \frac{A_{s_i}}{\sum_i A_{s_i}} \right]^{-1} A_{s_i} [T_{s_i}(t)^4 - T_{s_j}(t)^4] \quad (2.7)$$

$$F_{s_i, s_j} = \int_{s_j} \cos \theta_p \cos \theta_s \pi^{-1} S_{s_i, s_j}^{-2} ds_j \quad (2.8)$$

as derived from the Stefan-Boltzmann law [?, ?] wherefore ϵ_{s_i} and ϵ_{s_j} are the emissivity of surfaces s_i and s_j respectively, F_{s_i, s_j} is radiant-interchange configuration factor [?] between surfaces s_i and s_j , A_{s_i} and A_{s_j} are the areas of surfaces s_i and s_j respectively, σ is the Stefan-Boltzmann constant [?] and T_{s_i} and T_{s_j} are the surface temperature of surfaces s_i and s_j respectively.

The above description of longwave radiation as mentioned above for a room or thermal zone results in the necessity of a very detailed input, i.e. the configuration between all needs to be described by their shape, position and orientation in order to define F_{s_i, s_j} , and difficulties to introduce windows and internal gains in the zone of interest. Simplification is achieved by means of a ΔY or *delta-star transformation* [?] and by definition of a (fictive) radiant star node in the zone model. Literature [?] shows that the overall model is not significantly sensitive to this assumption. The heat exchange by longwave radiation between surface s_i and the radiant star node in the zone model can be described as

$$Q_{s_i,rs}(t) = \sigma \left[\frac{1 - \epsilon_{s_i}}{\epsilon_{s_i}} + \frac{A_{s_i}}{\sum_i A_{s_i}} \right]^{-1} A_{s_i} [T_{s_i}(t)^4 - T_{rs}(t)^4] \quad (2.9)$$

where ϵ_{s_i} is the emissivity of surface s_i , A_{s_i} is the area of surface s_i , $\sum_i A_{s_i}$ is the sum of areas for all surfaces s_i of the thermal zone, σ is the Stefan-Boltzmann constant [?] and T_{s_i} and T_{rs} are the temperatures of surfaces s_1 and the radiant star node respectively.

Shortwave radiation. Absorption of shortwave solar radiation on the interior surface is handled equally as for the outside surface. Determination of the receiving solar radiation on the interior surface after passing through windows is dealt with in the zone model.

2.1.4 Model extension for windows

The thermal model of a is similar to the model of an exterior wall but includes the absorption of solar irradiation by the different glass panes, the presence of gas gaps between different glass panes and the transmission of solar irradiation to the adjacent indoor zone.

Gap heat transfer. The total convective and longwave heat transfer through thin gas gaps as present in modern glazing systems is described as

$$Q_{net}(t, x) = A\lambda(x)d(x)^{-1}Nu(t, x)[T_{s_1}(t) - T_{s_2}(t)] + A\sigma\epsilon_{s_1}\epsilon_{s_2}[1 - (1 - \epsilon_{s_1})(1 - \epsilon_{s_2})]^{-1}[T_{s_1}^4(t) - T_{s_2}^4(t)] \quad (2.10)$$

where A is the glazing surface, $d(x)$ is the gap width, $Nu(t, x)$ is the Nusselt number of the gas, ϵ_{s_i} is the longwave emissivity of the surfaces and T_{s_i} is the surface temperature.

The Nusselt number of the present gas in the gap describing the ratio of convective to conductive heat transfer is generally described is

$$Nu(t, x) = n_1(t, x)Gr(t, x)^{n_2(t, x)} \quad (2.11)$$

$$Gr(t, x) = g\beta\rho^2d(x)^3\mu^{-2}[T_{s_1}(t) - T_{s_2}(t)] \quad (2.12)$$

where $Gr(t, x)$ is the Grashof number approximating the ratio of buoyancy to viscous force acting on the window gap gas, g is the gravitational acceleration, β is the coefficient of thermal expansion, ρ is the gas density, μ is the gas viscosity and $n_i(t, x)$ are correlation coefficients. These parameters $\{n_1, n_2\}$ are identical to $\{1.0, 0\}$ for all $Gr(t, x)$ below 7.10^3 , $\{0.0384, 0.37\}$ for all $Gr(t, x)$ between 10^4 and 8.10^4 , $\{0.41, 0.16\}$ for all $Gr(t, x)$ between 8.10^4 and 2.10^5 and $\{0.0317, 0.37\}$ for all $Gr(t, x)$ above 2.10^5 .

Shortwave optical properties. The properties for absorption by and transmission through the glazing are taken into account depending on the angle of incidence of solar irradiation and are based on the output of the WINDOW 4.0 software [?, ?] as validated by Arasteh [?] and Furler [?]. Within this software, the angular dependence of the optical properties is determined based on the model of Furler [?]. The reflectivity r and transmissivity $t = 1 - r$ are determined with the Fresnel equations [?] and Snell's Law of refraction [?], based on the relative refractive index n as follows

$$r(t, x) = 0.5 \sin^2 (\xi(t, x) - \xi'(t, x)) \sin^{-2} (\xi(t, x) + \xi'(t, x)) + 0.5 \tan^2 (\xi(t, x) - \xi'(t, x)) \tan^{-2} (\xi(t, x) + \xi'(t, x)) \quad (2.13)$$

where $\sin \xi(t, x) = n \sin \xi'(t, x)$. The resulting transmittance $T(t, x)$ and reflectance $R(t, x)$ for a single glass pane after multiple reflections is obtained from

$$T(t, x) = t_0^2 e^{-\alpha(x)d(x)/\cos \xi(t, x)} \left[1 - r(t, x)^2 e^{-\alpha d(x)/\cos \xi(t, x)} \right]^{-1} \quad (2.14)$$

$$R(t, x) = r(t, x) \left[1 + T(t, x) e^{-\alpha(x)d(x)/\cos \xi(t, x)} \right] \quad (2.15)$$

where $d(x)$ is the thickness of the pane and $\alpha(x)$ is absorption coefficient. The total transmittance $T(t, x)$ and the absorptances $A_n(t, x)$ for multipane windows are retrieved using iterative equations taking into account the multiple internal reflections within the glazing system.

The resulting output from WINDOW 4.0 [?] depicts an array of the transmittances T through the window and the absorptances A_n for each glass pane n for $\xi_s \in \{(k/18)\}$ with $k \in \{0, 1, \dots, 9\}$. The same array input is used in other dynamic building simulation tools, e.g. in TRNSYS [?] where values for different angles are retrieved by means of linear interpolation.

2.1.5 Model extension for ground slabs

The heat flow through building envelope constructions in contact with a is the same for the interior surface and the conduction process, but differs at the exterior surface in contact with the ground. As the heat transfer through the ground is 3-dimensional and defined by a large time lag, the exterior surface heat balance is generally approximated based on ISO 13370.

The total heat flow through the ground is given by

$$Q_{net}(t, x) = L_S(x) [\bar{T}_i - \bar{T}_e] - L_{pi}(x) \hat{T}_i \cos \gamma_i(t) + L_{pe}(x) \hat{T}_e \cos \gamma_e(t) \quad (2.16)$$

where L_S is the steady-state thermal coupling coefficient, L_{pi} and L_{pe} are the internal and external periodic thermal coupling coefficients respectively, \bar{T} is the annual average temperature, \hat{T} is the annual average temperature amplitude, and γ_i and γ_e determine the time lag of the heat flow cycle compared with that of the internal and external temperature respectively.

The steady-state and periodic thermal coupling coefficient area is determined as

$$L_S(x) = A(x) \frac{\lambda_g(x)}{0.457B_t(x) + d_t(x) + 0.5z} + zP(x) \frac{2\lambda_g}{\pi z} \left[1 + \frac{0.5d_t(x)}{d_t(x) + z} \right] \ln \left[\frac{z}{d_t} + 1 \right] \quad (2.17)$$

$$L_{pi}(x) = A(x) \frac{\lambda_g(x)}{d_t(x)} \sqrt{\frac{2}{\left[1 + \frac{\delta}{d_t(x)} \right]^2 + 1}} ; L_{pe}(x) = 0.37P(x) \lambda_g(x) \ln \left[\frac{\delta}{d_t(x)} + 1 \right] \quad (2.18)$$

where $A(x)$ is the wall area, λ_g is the thermal conductivity of the unfrozen ground, $B_t(x)$ is the characteristic dimension of the floor, $d_t(x)$ is the equivalent thickness of the wall construction, z is the depth of the wall (i.e. floor) below ground level, δ is periodic penetration depth (i.e. the depth in the ground at which the temperature amplitude is reduced to e^{-1} of that at the surface) and $P(x)$ is the exposed perimeter of the wall. The angle $\gamma_e(t)$ is determined as $2\pi t/t_{yr} + \pi/12 - \arctan d_t(x)/(d_t(x) + \delta)$ and $\gamma_e(t)$ is determined as $2\pi t/t_{yr} + \pi/12 + 0.22 \arctan \delta/(d_t(x) + 1)$.

2.2 Zone model

Consisting of both the convective as radiative calculation for determination of thermal comfort.

2.2.1 Thermal response model

Also the thermal response of a can be divided into a convective, longwave radiative and shortwave radiative process influencing both thermal comfort in the depicted zone as well as the response of adjacent wall structures.

Convective. The air within the zone is modeled based on the assumption that it is well-stirred, i.e. it is characterized by a single uniform air temperature. This is practically accomplished with the mixing caused by the air distribution system. The convective gains and the resulting change in air temperature T_a of a single thermal zone can be modeled as a thermal circuit. The resulting heat balance for the air node can be described as

$$\begin{aligned} \frac{\partial T_a}{\partial t} c_a V_a = & \sum_i^N Q_{i,a}(t) + \sum_i^{n_s} R_{s,ci}^{-1} A_{s,i} [T_a(t) - T_{s,i}(t)] + \sum_i^{n_z} \dot{m}_{a,z}(t) [h_a - h_{a,z}] \\ & + \dot{m}_{a,e} [h_a(t) - h_{a,e}(t)] + \dot{m}_{a,sys}(t) [h_a(t) - h_{a,sys}(t)] \end{aligned} \quad (2.19)$$

wherefore the specific air enthalpy h_a is determined as $c_a \vartheta_a + \chi_a c_w \vartheta_a + \chi_a h_{w,ev}$ and where T_a is the air temperature of the zone, c_a is the specific heat capacity of air at constant pressure, V_a is the zone air volume, Q_a is a convective internal load, $R_{s,i}$ is the convective surface resistance of surface s_i , $A_{s,i}$ is the area of surface s_i , $T_{s,i}$ the surface temperature of surface s_i , $\dot{m}_{a,z}$ is the mass flow rate between zones, $\dot{m}_{a,e}$ is the mass flow rate between the exterior by natural infiltration, $\dot{m}_{a,sys}$ is the mass flow rate provided by the ventilation system, ϑ_a is the air temperature in degrees Celsius, χ_a is the air humidity ratio, c_w is specific heat of water vapor at constant pressure and $h_{w,ev}$ is evaporation heat of water at 0 degrees Celsius.

Infiltration and ventilation systems provide air to the zones, undesirably or to meet heating or cooling loads. The thermal energy provided to the zone by this air change rate can be formulated from the difference between the supply air enthalpy and the enthalpy of the air leaving the zone h_a . It is assumed that the zone supply air mass flow rate is exactly equal to

the sum of the air flow rates leaving the zone, and all air streams exit the zone at the zone mean air temperature. The moisture dependence of the air enthalpy is neglected in most cases.

A multiplier for the zone capacitance $f_{c,a}$ is included. A $f_{c,a}$ equaling unity represents just the capacitance of the air volume in the specified zone. This multiplier can be greater than unity if the zone air capacitance needs to be increased for stability of the simulation. This multiplier increases the capacitance of the air volume by increasing the zone volume and can be done for numerical reasons or to account for the additional capacitances in the zone to see the effect on the dynamics of the simulation. This multiplier is constant throughout the simulation and is set to 5.0 if the value is not defined.

Longwave radiation. The exchange of longwave radiation in a zone has been previously described in Sect. 2.1.3 by Eq. 2.5 and further considering the heat balance of the interior surface. Here, an expression based on *radiant interchange configuration factors* of *view factors* is avoided based on a delta-star transformation and by definition of a *radiant star temperature* T_{rs} . Literature [?] shows that the overall model is not significantly sensitive to this assumption. This T_{rs} can be derived from the law of energy conservation in the radiant star node as $\sum_i Q_{s_i-rs}$ must equal zero. Long wave radiation from internal sources are dealt with by including them in the heat balance of the radiant star node resulting in a diffuse distribution of the radiative source¹.

Shortwave radiation. Transmitted shortwave solar radiation is distributed over all surfaces in the zone in a prescribed scale. This scale is an input value which may be dependent on the shape of the zone and the location of the windows, but literature [?] shows that the overall model is not significantly sensitive to this assumption.

2.2.2 Thermal comfort

For thermal measures, both the determination of an *operationally* or *dry resultant temperature* ϑ_c as well as the *predicted mean vote* (PMV) and *predicted percentage of dissatisfied* (PPD) are implemented.

Operationally temperature. A *dry resultant temperature* ϑ_c can be defined based on the previous assumptions for convective heat exchange, radiation and internal gains as

$$\vartheta_c(t) = \left[\vartheta_{mrt}(t) + \vartheta_a(t) \sqrt{10v_a(t)} \right] \left[1 + \sqrt{10v_a(t)} \right]^{-1} \quad (2.20)$$

which can be approximated by $0.5[\vartheta_{mrt} + \vartheta_a]$, $\forall v_a \leq 0.1 \text{ m/s}$ where ϑ_{mrt} and ϑ_a depict the mean radiative and air temperature respectively and v_a is the air velocity. Here, ϑ_{mrt} is determined as the area weighted surface temperature of the zone surfaces.

Comfort indicators. Most meaningful for expression the thermal environment is to state what percentage of persons can be expected to be decidedly dissatisfied. The *predicted percentage of dissatisfied* (PPD) [?] can be expressed as

¹ Note that, as a result, the radiant star temperature T_{rs} is not equal to the radiative temperature of the zone as will be perceived by occupants.

$$PPD = 100 - 95 e^{-0.003353 PMV^4 - 0.2179 PMV^2} \quad (2.21)$$

as function the *predicted mean vote* (PMV) [?] which expresses the thermal person of persons in the commonly used psycho-physical ASHRAE scale between -3 and +3 [?]. The expression for PMV can be defined [?, ?] as

$$\begin{aligned} PMV = & \left[0.303 e^{-0.036 M_A} + 0.028 \right] \left[M_A - 3.96 \cdot 10^{-8} f_{cl} [T_{cl}^4 - T_{mrt}^4] - f_{cl} h_c [T_{cl} - T_a] \right. \\ & - 3.05 [5.73 - 0.007 M_A - p_{vp}] - 0.42 [M_A - M_{eq}] - 0.0173 M_A [5.87 - p_{vp}] \\ & \left. - 0.0014 M_A [34 - \vartheta_a] \right] \end{aligned} \quad (2.22)$$

where M_A is the specific metabolic rate per body surface area of the human body, M_{eq} is the metabolic equivalent task equal to 58.15 Wm^{-2} , p_{vp} is the partial water vapor pressure, T_a is the air temperature, T_{cl} is the surface temperature of clothing, f_{cl} is the clothing area factor, T_{cl} is the mean radiant temperature and h_c is the convective heat transfer. The required clothing temperature T_{cl} can be determined as

$$T_{cl} = T_b - 0.0028 M_A - R_{cl} [3.96 \cdot 10^{-8} f_{cl} [T_{cl}^4 - T_{mrt}^4] + f_{cl} h_c [T_{cl} - T_a]] \quad (2.23)$$

where T_b is the body temperature equal to 308.95 K , R_{cl} depicts the thermal resistance from the skin to the outer surface of the clothed body and is equal to $0.155 I_{cl}$ where I_{cl} is the so-called the *clo-value*, and where f_{cl} is determined as $1.05 + 0.1 I_{cl}$ if $I_{cl} > 0.5$ or $1.00 + 0.2 I_{cl}$ elsewhere.

2.3 Initial value problem

Chapter 3

Thermal building system

Roel De Coninck and Lieve Helsen

Abstract A numeric thermal system model is developed in Modelica for integrated energy simulation.

Chapter 4

Electricity system

Juan Van Roy, Bart Verbruggen and Johan Driesen

Abstract A numeric electric system model is developed in Modelica for integrated energy simulation.

Part II

Validation or verification

val-i-dation (n.) 1. To declare or make legally valid. 2. To mark with an indication of official sanction. 3. To establish the soundness of; corroborate.

Chapter 5

Building energy simulation test - BESTEST

Ruben Baetens and Dirk Saelens

5.1 Introduction

The thermal building model are *validated* by comparative tests based on the *Building Energy Simulation Test* (BESTEST) [?, ?] as developed under supervision of the International Energy Agency (IEA) [?, ?] and standardized as the ANSI/ASHRAE Standard 140-2007 [?]. This standard consists of a series of specified test cases and has been developed to diagnose whole building energy simulation software. Here, output values such as the annual energy consumptions, peak loads, average and extreme room air temperatures, and some hourly data are compared to miscellaneous building energy simulation programs, e.g. BLAST, DOE2.1D, ESP-R, SERIRES / SUNCODE, S3PAS, TASE and TRNSYS.

5.1.1 Building energy simulation test cases

Within this work, the so-called *basic test cases* are used to *validate* the building model. These test cases test the ability to model combined effects as thermal mass, solar gains and solar shading, air infiltration, internal heat gains, sunspaces and thermostat control. Three series of basic cases are tested :

1. Qualification cases 600 to 650 representing a set of lightweight buildings that are relatively realistic with respect to their thermal characteristics. Within this set of cases, case 600 tests the south solar transmission, case 620 tests the east and west solar transmittance and incidence, case 640 tests night setback and case 650 tests venting.

Ruben Baetens

K.U.Leuven, Kasteelpark Arenberg 40 bus 2447, BE-3001 Leuven (Heverlee) e-mail: ruben.baetens@bwk.kuleuven.be

Dirk Saelens

K.U.Leuven, Kasteelpark Arenberg 40 bus 2447, BE-3001 Leuven (Heverlee) e-mail: dirk.saelens@bwk.kuleuven.be

2. Qualification cases 900 to 960 representing a set of heavyweight buildings that are relatively realistic with respect to their thermal characteristics and include a building configuration with a sunspace. Within this set of cases, case 900 tests the thermal mass and solar interaction, test 920 tests the east and west transmittance and its mass interaction, case 940 tests night set-back and its mass interaction, case 950 tests venting and its mass interaction and case 960 tests passive solar and interzonal heat transfer.
3. Free-float basic test cases 600FF, 900FF, 650FF and 950FF equaling the corresponding non-FF cases except the absence of a mechanical heating or cooling systems.

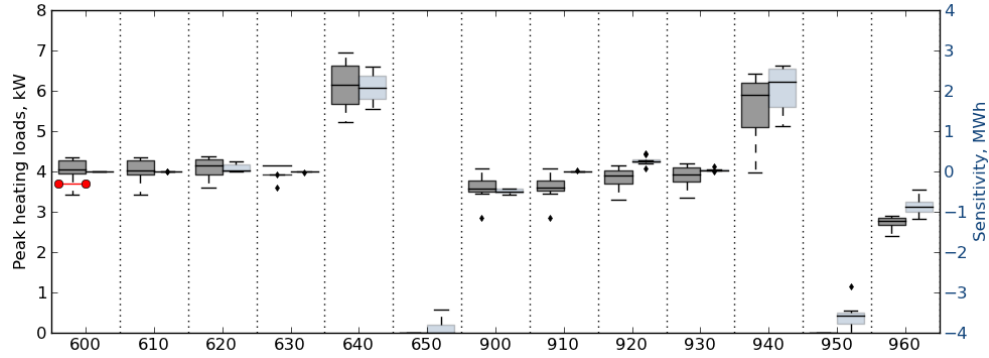
5.1.2 Test results

5.1.2.1 Annual heating and cooling loads

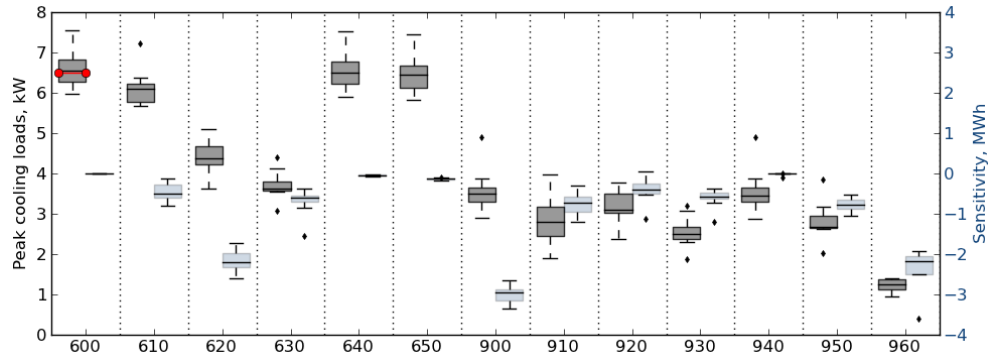


Fig. 5.1 Annual heating and sensible cooling loads for the low mass and heavy mass buildings.

5.1.2.2 Peak heating and cooling loads



(a) Peak heating loads for the low mass and heavy mass buildings.



(b) Peak sensible cooling loads for the low mass and heavy mass buildings.

Fig. 5.2 Peak heating and sensible cooling loads for the low mass and heavy mass buildings.

5.1.2.3 Indoor air temperatures

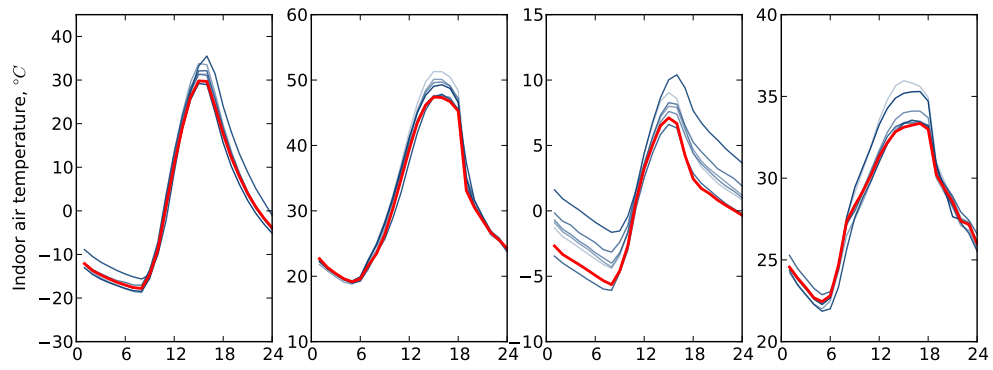


Fig. 5.3 Indoor temperatures for the low mass and heavy mass buildings.

Chapter 6

Thermal building energy system test - BESTEST

Roel De Coninck and Lieve Helsen

Abstract A numeric thermal system model is developed in Modelica for integrated energy simulation.

Chapter 7

IEEE Distribution system analysis for radial test feeders

Juan Van Roy, Bart Verbruggen and Johan Driesen

Abstract A numeric electric system model is developed in Modelica for integrated energy simulation.

Part III
Literature

lit-er-a-ture (n.) 1. The body of written works of a language, period, or culture. 2. Imaginative or creative writing, especially of recognized artistic value: "Literature must be an analysis of experience and a synthesis of the findings into a unity" (Rebecca West). 3. The art or occupation of a literary writer. 4. The body of written work produced by scholars or researchers in a given field: medical literature. 5. Printed material: collected all the available literature on the subject. 6. Music All the compositions of a certain kind or for a specific instrument or ensemble: the symphonic literature.

Bibliography

Index

comfort, 16

ground slab, 14

wall, 9, 11, 14

window, 13

zone, 9, 15